Printed ISSN 1330–0016
Online ISSN 1333–9133
CD ISSN 1333–8390
CODEN FIZBE7

COULOMB GAUGE QCD AND THE EXCITED HADRON SPECTRUM

FELIPE LLANES-ESTRADA[a], STEPHEN R. COTANCH [b], TIM VAN CAUTEREN[a], JUAN M. TORRES-RINCON[a], PEDRO BICUDO[c] and MARCO CARDOSO[c]

[a]*Depto. Física Teórica I, Universidad Complutense de Madrid, 28040 Madrid, Spain*

[b]*Department of Physics, North Carolina State University, Raleigh, NC 27695, U. S. A.*

[c]*Instituto Superior Tecnico, Avda. Rovisco Pais 1096, Lisbon, Portugal*

Received 28 December 2010; Accepted 26 October 2011
Online 5 January 2012

We discuss progress in understanding the light- and heavy-quark excited hadron spectrum from Coulomb gauge QCD. For light-quark systems, we highlight the insensitivity to spontaneous chiral symmetry breaking, which predicts Wigner parity-degeneracy in the highly-excited hadron spectrum and allows the quark-mass momentum dependence to be experimentally probed. For heavy-quark meson decays, we invoke the Franck-Condon principle, a consequence of small velocity changes for heavy quarks, to extract qualitative, but model-independent, structure insight from the momentum distribution of the decay products.

PACS numbers: 11.30.Rd, 12.38.Lg, 12.39.Mk, 12.40.Vv, 12.40.Yx UDC 539.126

Keywords: excited hadron spectrum, light-quark and heavy-quark systems, Coulomb gauge QCD, spontaneous chiral symmetry breaking, Franck-Condon principle

1. *Motivation for Coulomb gauge QCD studies*

Recent years have witnessed steady progress in both understanding and applying quantum chromodynamics (QCD) in the Coulomb gauge. Much attention has been formal, focusing on the such issues as the behavior of the Green's function in the deep infrared [1], the Slavnov-Taylor identities [2] necessary for a complete renormalization treatment in this gauge and the structure of the ground state vacuum [3]. In this paper, the thrust is more phenomenological as we detail how an approximate Coulomb gauge formulation [4] can provide important hadron structure insight. While the QCD treatment is not rigorous, we have been able to identify several fundamental issues which a more precise Coulomb gauge QCD analysis can resolve.

In addition to the advantages of Coulomb gauge QCD, it is also worthwhile to comment on this formulation's major limitation involving calculating observables that connect different reference frames. Since the Coulomb condition, $\nabla \cdot \mathbf{A}^a = 0$, is specified for one chosen frame (typically the hadron center of momentum), the computation of a form factor or an electromagnetic transition matrix element, which requires hadron wavefunctions in two different frames, entails employing boost operators [5]. This introduces a formidable difficulty since in this gauge, these operators are as complicated as the exact Hamiltonian. Although one can adapt methods developed for the relativistic quark model [6], unambiguous, reliable results become very difficult to obtain. Related, fragmentation functions and parton distribution functions, more conveniently calculated in light-front quantization, are also difficult to formulate in the Coulomb gauge.

In contrast, Coulomb gauge QCD is much more ideal for spectroscopy and hadron structure, including the vacuum which is difficult for light cone formulations. Solving the equation of motions variationally, either on the lattice or by approximate model truncation, allows study of the entire spectrum with masses of arbitrary excitations (in the rest frame), any spin and all other quantum numbers. The variational treatment is possible because this gauge is physical (contains no spurious degrees of freedom or ghosts), involving only transverse gluons. Gauss' law, which is essential for confinement, is explicitly satisfied and incorporated as a constraint. However, the resulting interaction kernel is complicated. Fortunately, with insight provided by lattice QCD, it is amenable to modeling using a more calculable confining kernel containing a linear potential as used in Ref. [4] and further supported by other approaches [7]. This approximate framework provides several new insights into the structure of highly-excited mesons and baryons. One is the role of chiral symmetry for the complete hadron spectrum. As detailed in Section 2, because chiral symmetry is incorporated (unlike constituent-quark-model formulations), one can clearly understand why the light-quark, low-mass pseudoscalar mesons are strongly governed by spontaneous chiral symmetry breaking, while the high lying spectrum is insensitive to chiral symmetry breaking leading to parity doublets. This is difficult to explain with other methods which generally do not respect chiral symmetry and/or can not predict the excited spectrum. For example, for heavy quarks, non-relativistic QCD (NRQCD) [8] reasonably describes the low-lying spectrum. However, it becomes inadequate for strongly-excited states due to the attending large quark momenta. Again, the Coulomb gauge formulation naturally extends to systems involving arbitrary large momenta. Further, in addition to mass spectra, one can also learn about the momentum structure of the hadrons in strong decays, due to the large scale provided by the heavy-quark mass and high momentum, $m_Q v \gg \Lambda_{\rm QCD}$, which is discussed in Section 3. This provides decay signatures which may be useful for identifying exotic hadrons and is analogous to the Franck-Condon principle of molecular physics. Section 4 discusses new insights through future measurements at Jefferson Lab with the anticipated 12 GeV upgrade. Finally, a summary of key results provided in this paper is presented in Section 5.

2. *Insight into chiral symmetry*

Chiral symmetry is said to be hidden (or spontaneously broken) by the condensation of quarks in the ground state (vacuum) of QCD. This feature, documented in both Landau and Coulomb gauge studies, is expected to be of lesser importance in the excited spectrum as illustrated by a simple analogy. Consider two identical solid-bridge supporting pillars in two different shallow ponds, one salt and the other fresh water (thus breaking the symmetry between them). Their net weight is essentially the same (approximately symmetrical) even though one experiences a slightly larger buoyant force from the salt water. Two highly excited, but opposite parity, hadrons are analogous to the two pillars since their quarks have (on average) large momenta but now the running quark mass is small [9], so chiral symmetry is approximately restored. The first statement, that the momentum is larger for excited states, is supported by the relativistic virial theorem [10] and also explicit variational model computations for momentum distributions as detailed in our Coulomb gauge approach [11, 12]. The second statement, that the running quark mass is small for large momentum, is a consequence of asymptotic freedom, well-known from early QCD studies [13].

An immediate consequence of chiral symmetry restoration is the reappearance of Wigner symmetry in the highly-excited spectrum, with doublet partner states of equal mass but opposite parity [14]. For three-quark configurations, relativistic chiral approaches like ours predict that states come in quartets, reducible representations that split into two doublets [15]. As an example, take the family of spin 1/2 excitations of the isospin 3/2 Δ. We have used the Cornell approach to Coulomb gauge QCD with harmonic oscillator interactions and a large, harmonic oscillator basis model space to diagonalize the Hamiltonian. All orthogonalizations and symmetrizations are performed numerically and the resulting Δ spectrum is plotted in Fig. 1 for the first 20 eigenvalues. Note that, while there are variations

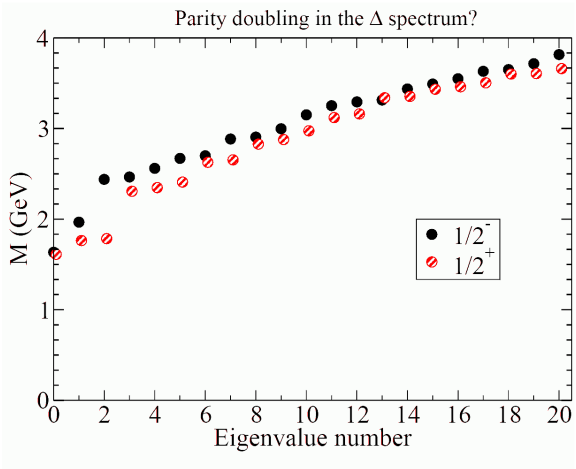

Fig. 1. Excited $I = 3/2$, $J = 1/2$ Δ spectrum. Parity doublets emerge, especially for higher excited states.

for the lower states, parity doubling is indeed a feature of the higher spectrum illustrating chiral symmetry in the Wigner mode. Lattice gauge simulations and also Dyson-Schwinger approaches have difficulties generating excited state spectra which is easily computed in Coulomb gauge based models.

A potential problem investigating parity doublets experimentally, especially if the spectrum is numerous, is to identify the correct corresponding Wigner partners. This is where theoretical calculations, which do not have this ambiguity, can be of great benefit as we again document in Fig. 2 where the doublet separation energy (splitting) is plotted for each J. The parity degeneracy clearly emerges for increasing excitation energy and J. This variational Monte Carlo investigation is still in progress and the results are preliminary.

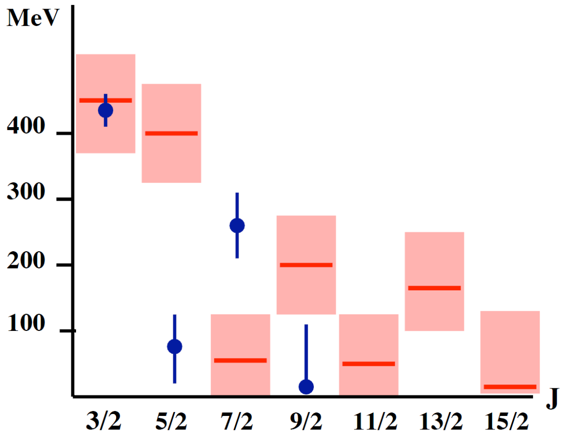

Fig. 2. Predicted baryon parity doublet splitting from variational Monte Carlo calculations (boxes) compared to data (solid circles) from Ref. [15].

Related, but perhaps more interesting, one can use the onset of this degeneracy to probe the quark-mass-momentum dependence (running) in the infrared. The quark mass in our approach appears both in the quark spinors and in the QCD Hamiltonian. For small quark mass and high momentum, a series expansion of the spinors and the Hamiltonian in the parameter $m(k)/k$ reveals several insights. Expanding the spinors

$$u_\lambda(\mathbf{k}) = \frac{1}{\sqrt{2E(k)}} \left[\begin{array}{c} \sqrt{E(k)+m(k)}\chi_\lambda \\ \sqrt{E(k)-m(k)}\,\boldsymbol{\sigma}\cdot\hat{\mathbf{k}}\chi_\lambda \end{array} \right], \tag{1}$$

yields the leading terms at high momentum

$$u_\lambda(\mathbf{k}) \to \frac{1}{\sqrt{2}} \left[\begin{array}{c} \chi_\lambda \\ \boldsymbol{\sigma}\cdot\hat{\mathbf{k}}\chi_\lambda \end{array} \right] + \frac{1}{2\sqrt{2}}\frac{m(k)}{k} \left[\begin{array}{c} \chi_\lambda \\ -\,\boldsymbol{\sigma}\cdot\hat{\mathbf{k}}\chi_\lambda \end{array} \right], \tag{2}$$

with $E(k) = \sqrt{k^2+m(k)^2}$. The first term is chirally invariant and the second chiral-symmetry breaking. Note that the lower components in each term have the opposite sign. Instead of directly expanding the QCD Hamiltonian, expand the Hamiltonian matrix elements computed in the Hilbert space spanning highly excited resonances, labeled n, where the average momentum, $\langle k\rangle$, is large

$$\left\langle n\middle|H^{QCD}\middle|n\right\rangle = \left\langle n\middle|H^{QCD}_{\chi_S}\middle|n\right\rangle + \left\langle n\middle|\frac{m(k)}{k}H^{QCD}_{\chi_B}\middle|n\right\rangle + \ldots \,. \tag{3}$$

Again, the first Hamiltonian term, labeled by χ_S, is chirally symmetric, while the second, labeled χ_B, is not and involves nonchiral, spin-dependent potentials in the quark-quark interaction.

Now recall for zero mass current quarks, the chiral charge,

$$Q_5 = \int \mathrm{d}\mathbf{x}\, \psi^\dagger(\mathbf{x})\gamma_5\psi(\mathbf{x}) \ , \tag{4}$$

commutes with the QCD Hamiltonian. Nevertheless, chiral symmetry is still spontaneously broken by the ground state vacuum since $Q_5|0\rangle \neq 0$, leading to a large constituent quark mass in the quark propagator, pseudoscalar Goldstone bosons and no parity-degeneracy in ground-state baryons. Insight about the chiral charge operator follows by performing a BCS transformation to a quasiparticle basis with operators B and D defined by

$$B_{\lambda\mathcal{C}}(\mathbf{k}) \quad = \quad \cos\frac{\theta_k}{2} b_{\lambda\mathcal{C}}(\mathbf{k}) - \lambda \sin\frac{\theta_k}{2} d^\dagger_{\lambda\mathcal{C}}(-\mathbf{k}) \tag{5}$$

$$D_{\lambda\mathcal{C}}(-\mathbf{k}) \quad = \quad \cos\frac{\theta_k}{2} d_{\lambda\mathcal{C}}(-\mathbf{k}) + \lambda \sin\frac{\theta_k}{2} b^\dagger_{\lambda\mathcal{C}}(\mathbf{k}) \ . \tag{6}$$

Then using the standard Fock operator normal mode representation for the quark field

$$\Psi(\mathbf{x}) = \sum_{\lambda\mathcal{C}} \int \frac{\mathrm{d}\mathbf{k}}{(2\pi)^3} [u_\lambda(\mathbf{k}) b_{\lambda\mathcal{C}}(\mathbf{k}) + v_\lambda(-\mathbf{k}) d^\dagger_{\lambda\mathcal{C}}(-\mathbf{k})] e^{\mathrm{i}\mathbf{k}\cdot\mathbf{x}} \hat{\epsilon}_{\mathcal{C}} \ , \tag{7}$$

and substituting for the bare spinors, the chiral charge can be expressed as

$$\begin{aligned} Q_5 \quad = \quad & \int \frac{\mathrm{d}\mathbf{k}}{(2\pi)^3} \sum_{\lambda\lambda'\mathcal{C}} \frac{k}{\sqrt{k^2+m^2(k)}} \\ & \times \Big[(\boldsymbol{\sigma}\cdot\hat{\mathbf{k}})_{\lambda\lambda'} \Big(B^\dagger_{\lambda\mathcal{C}}(\mathbf{k}) B_{\lambda'\mathcal{C}}(\mathbf{k}) + D^\dagger_{\lambda'\mathcal{C}}(-\mathbf{k}) D_{\lambda\mathcal{C}}(-\mathbf{k}) \Big) + \\ & \frac{m(k)}{k} (\mathrm{i}\sigma_2)_{\lambda\lambda'} \ \Big(B^\dagger_{\lambda\mathcal{C}}(\mathbf{k}) D^\dagger_{\lambda'\mathcal{C}}(-\mathbf{k}) + B_{\lambda'\mathcal{C}}(\mathbf{k}) D_{\lambda\mathcal{C}}(-\mathbf{k}) \Big) \Big] \ . \end{aligned} \tag{8}$$

The first two terms between the square brackets are quark and anti-quark number operators, i.e. operators conserving the number of particles, flipping spin and parity.

For $m(k) \ll k$, they dominate the third and fourth terms representing pion creation and annihilation. As argued in Ref. [12], repeated action of the chiral charge on a three-quark state produces a quartet of states, two of each parity, that dynamically split into two doublets of parity partners. Moreover, the mass splitting between partners is a direct measure of $m(k)$ and they are degenerate when $m(k)$ vanishes.

In order to link this parity doublet mass splitting, $\Delta M = |M^{P=+} - M^{P=-}|$, to the running quark mass, we examine the lowest-lying parity doublets for increasing spin J and incorporate the following key elements.

- Regge trajectories, $J = \alpha_0 + \alpha M^{\pm 2} \overset{J\to\infty}{\longrightarrow} \alpha M^{\pm 2}$.
- Relativistic virial theorem, $\langle k \rangle \to c_2 M^{\pm} \to \dfrac{c_2}{\sqrt{\alpha}}\sqrt{J}$.
- Canceling of the chirally invariant term, $\left\langle n|H_{\chi S}^{QCD}|n\right\rangle$, in ΔM so that $\Delta M \ll M^{\pm}$ and $\Delta M \to \left\langle \dfrac{m(k)}{k} H_{\chi B}^{QCD} \right\rangle \to c_3 \dfrac{m(\langle k \rangle)}{\langle k \rangle} \left\langle H_{\chi B}^{QCD} \right\rangle$.
- In $H_{\chi S}^{QCD}$, the spin-orbit term, $\mathbf{L}\cdot\mathbf{S}$, is crucial to correct the angular momentum in the centrifugal barrier from $\mathbf{L}^2$ to the chirally invariant $\mathbf{L}^2 + 2\mathbf{L}.\mathbf{S} = \mathbf{J}^2 - \frac{3}{4}$. Due to the sign difference in the helicity-dependent term, $-\sigma\cdot\hat{\mathbf{k}}$, in the spinor, the spin-orbit term in $H_{\chi B}^{QCD}$ adds to the mass splitting instead of cancelling out as it does for $H_{\chi S}^{QCD}$. Since the centrifugal barrier scales like $M^{\pm}$ for high J, the spin-orbit term scales with one less power of J
$$\left\langle H_{\chi B}^{QCD} \right\rangle \to c_5 M^{\pm} J^{-1} \to \frac{c_5}{\sqrt{\alpha}}\sqrt{\frac{1}{J}} \ .$$

Combining these elements yields
$$\Delta M \to \frac{c_3 c_5}{c_2} m(\langle k \rangle) J^{-1} \ . \tag{9}$$

This equation linearly relates the parity splitting (an observable) to the running of the quark mass at the average momentum $\langle k \rangle$ for that splitting. Note that $\langle k \rangle$ will vary with splitting, increasing for higher excited states (and J). Although there are still unknown constants that are gauge dependent, a useful power-law running of $m(\langle k \rangle)$ (or equivalently $m(k)$) can be obtained model-independently from data at high spin J by fitting the splitting to the form $\Delta M \propto J^{-i}$ and determining the exponent i. Then, the power-law behaviour of the running quark mass is given by
$$m(k) \propto k^{-2i+2} \ . \tag{10}$$

As indicated in Fig. 2, the known masses of lowest-lying Δ resonances for $J = 1/2, \cdots, 15/2$ are currently not sufficient to derive this exponent. Establishing the masses of the parity doublets for spins $J > 9/2$ would resolve this and provide a running quark mass momentum dependence as schematically indicated in Fig. 3.

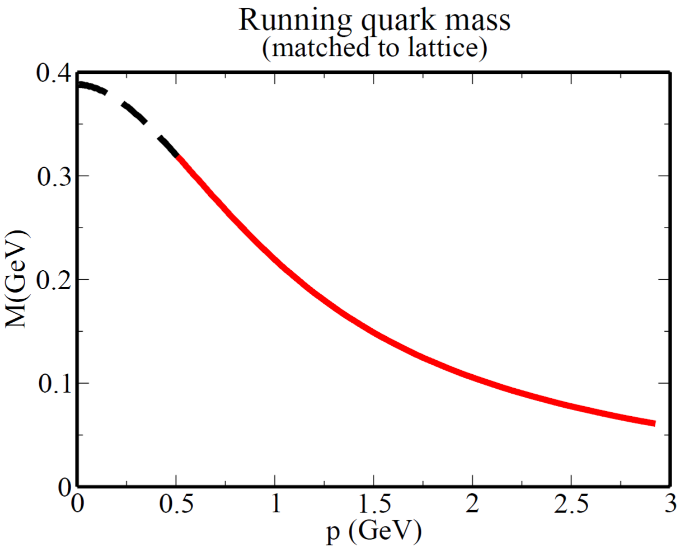

Fig. 3. Cartoon showing the running quark mass as a function of momentum. The solid line is a power law whose exponent can be obtained from the decreasing parity doublet splittings for increasing J, as illustrated in Fig. 2.

3. Franck-Condon principle and heavy hadron decays

In general, calculating most hadron observables such as masses, widths, or partial branching ratios, entails integrating over quark momenta which precludes direct, experimental study of momentum distributions. Here, we submit that it is possible to access this distribution by measuring the decay hadron momenta of open flavor, light-heavy quark $q\bar{Q}$ and $\bar{q}Q$ systems from highly excited heavy quarkonium $Q\bar{Q}$ states. This assertion is based on two points. The first is that $Q\bar{Q}$ states with high excitation energies also have high momenta. The second is the heavy-quark "velocity superselection rule" which states that in heavy-quark meson decays the velocity of the heavy quark is conserved and not affected by the non-heavy degrees of freedom (light quarks and gluons). This selection rule is a common ingredient in heavy-quark effective theories such as HQET and NRQCD and is due to the clear scale separation between the large mass of the heavy quark and Λ_{QCD} (as well as the running masses of light quarks). In particular, the NRQCD Lagrangian at leading order in Λ_{QCD}/m_Q for heavy quarkonium is

$$\mathcal{L}_{LO} = \left(\begin{array}{cc} \overline{h}_v^{(+)}, & \overline{h}_w^{(-)} \end{array} \right) \left(\begin{array}{cc} \mathbf{i}\mathbf{v}\cdot\boldsymbol{\nabla} - \frac{\nabla^2}{2m_Q} & 0 \\ 0 & \mathbf{i}\mathbf{w}\cdot\boldsymbol{\nabla} - \frac{\nabla^2}{2m_Q} \end{array} \right) \left(\begin{array}{c} h_v^{(+)} \\ h_w^{(-)} \end{array} \right), \qquad (11)$$

where the velocities, v and w, are the same for the quark creation and destruction operators, $h^{(\pm)}$. It is clear that the operator structure of this Lagrangian preserves the heavy-quark velocity. Coulomb gauge QCD also takes this form in the heavy-quark limit as can be seen from the explicit Hamiltonian [4].

Returning to accessing quark momentum distributions and invoking these two principles for a highly excited $Q\bar{Q}$ decay to open flavor mesons, $\to \bar{q}Qq\bar{Q}$, in leading order, the velocity (and momentum) of each heavy quark is the same before and after the decay. Then the quarkonium momentum distribution is approximately given by the momentum of the final state mesons containing the heavy quarks, which is directly measurable. This only applies to 3 or 4-body final states since 2-body final states have fixed momentum due to over all momentum conservation. Technically, in the limit of infinite heavy-quark mass, these principles, combined with momentum conservation, would forbid a two-body final state decay. This implies that for finite mass, decays to two-body states should be suppressed relative to three or more hadron final states. The above decay features should therefore be more pronounced in bottomonium transitions compared to charmonium decays.

This effect [16] is very similar to the well-known Franck-Condon principle in molecular physics. It states that during an electronic transition, the nuclear degrees freedom (position and momentum) are essentially frozen due to the large scale difference between the electron and nucleon masses. Therefore, the wavefuncion associated with the motion of the nuclei remains the same after the transition.

It is thus possible to reconstruct the excited state quarkononium wavefunction by measuring the final state heavy-meson momentum distribution. In particular, a highly-excited pure $Q\overline{Q}$ state has a definite structure of Sturm-Liouville zeroes (nodes) in the wave function, whereas a $Q\bar{Q}g$ hybrid state (that is, quarkonium plus a gluonic excitation) with the same mass, say in the ground state, would have no Sturm-Liouville zeroes (no nodes). Experiment can now distinguish between these two hadron structures.

As an illustrative example, consider the decay of $\Upsilon(10860)$ to $B_s\,\overline{B}_s$ and $B_s^*\,\overline{B}_s^*$ final states. This parent state is generally accepted as an excited two-body quarkonium configuration, i.e. having several nodes. The momentum distribution for this state was calculated [16] using a Coulomb gauge model $5S$ wavefunction having four nodes and is plotted in Fig. 4. Also plotted (dotted line) is the same distribution, but now a decay mechanism is included ($^3P_0$ scalar model). Both distributions have also been multiplied by phase space factors and exhibit a clear node structure (depicting additional nodes requires a non-linear graph). Also plotted is the recent Belle Collaboration data [17] for $\Upsilon(10860)$ decay to $B_s\,\overline{B}_s$ and $B_s^*\,\overline{B}_s^*$ including 2-, 3- and 4-body final meson states. Notice that there is reasonable agreement, especially the correspondence for the first Sturm-Liouville zero, affirming the validity of the Frank-Condon principle for heavy quark systems.

Finally, one can also construct a different momentum signature to distinguish between $Q\overline{Q}g$ hybrid candidates and possible tetraquark states with similar mass (both without Sturm-Liouville zeroes). Now it is necessary to study four-meson decays such as $Z \to D\overline{D}D\overline{D}$, or $D\overline{K}K\overline{D}$ for which one can obtain, from the momentum distribution in the final state, the off-plane correlator,

$$\Pi(\mathbf{p_1},\mathbf{p_2},\mathbf{p_3},\mathbf{p_4}) = \frac{|(\mathbf{p_1}\times\mathbf{p_2})\cdot\mathbf{p_3}|^{\mathbf{2}}}{\prod\limits_{i,j=1,\ i\neq j}^{\mathbf{4}} [|\mathbf{p_i}\times\mathbf{p_j}|]^{\mathbf{1/2}}}\ , \tag{12}$$

that reflects a distinctive non-planar structure from momenta combinations not present in 2-body or 3-body states. Consult Ref. [16] for a more complete discussion on using this signature to identify tetraquark states.

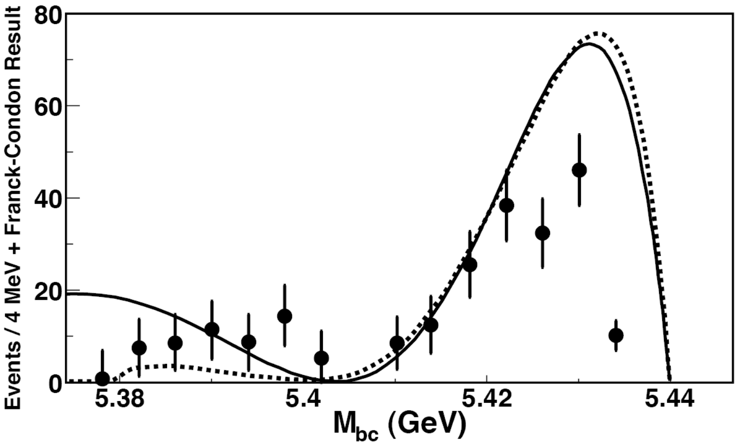

Fig. 4. Decay widths for $\Upsilon(10860)$. Solid line: predicted momentum distribution using the Frank-Condon principle for a 5S quarkonium wavefunction multiplied by phase space factors. Dotted line is the same as solid but now a decay mechanism is included. The dip in the data (dots) [17] is correlated with the first node in the momentum distribution.

4. Future excited-spectrum studies at Jefferson Lab

As discussed at this conference, one of the goals for the 12 GeV upgrade of CEBAF is to explore the highly-excited meson and baryon spectrum with existing experimental halls also having upgraded instrumentation. This will facilitate electroproduction measurements of excited baryon resonances with higher spins, J, allowing completion of the analysis involving Eq. 10. Further, finding these excited states will bring closure to quark models which have long predicted their existence. There is also a QCD motivation, to understand the onset of chiral symmetry breaking in the low spectrum, by clearly linking $m(k)$ from the asymptotically-free regime to the constituent quark mass. This is possible because m/k is a small parameter in the excited spectrum.

Equally, if not more, important is the construction of the new Hall D to conduct Glue-X experiments to search for exotic hadrons with gluonic degrees of freedom. This hall will also permit exploring the excited-meson spectrum, complementing the other halls in this endeavor. Since discovering exotica is a major goal of Glue-X, having a constraint on momentum distributions would be very useful and this may be possible again using the Frank-Condon principle. Consider for example the $\phi(2170)$ observed in electron-positron collisions by BaBar in the reaction

$$e^-e^+ \to \phi(2170) \to \phi f_0(980)\gamma \ .$$

Jefferson Lab will be able to produce it via $\gamma p \to \phi(2170)p$. Since this resonance has many open decay channels (K^+K^-, $K^+K^-\pi\pi$, etc), measuring the momentum of the two charged kaons may be useful to gain insight regarding the momentum distributions of the strange quarks in $\phi(2170)$. This would permit testing the presumed $3S$ quark model assignment (two Sturm-Liouville zeroes), or even documenting possible exotic components. Although the strange quark mass, m_s, is now comparable to the strong interaction strength, $\Lambda_{\rm QCD}$, the separation scale might still be sufficient for qualitative insight since the strange quark momentum, $p = m_s v/\sqrt{1-v^2/c^2}$, is large according to the relativistic virial theorem.

5. *Summary*

As discussed in the previous pages, the Coulomb gauge formulation of QCD has several advantages and provides an opportunity for dynamical insight regarding hadron structure. While not readily amendable for form factor predictions, it provides a natural framework for spectroscopic studies for highly-excited states as well as exotic configurations involving explicit gluonic degrees of freedom. The role of chiral symmetry has been clarified, both for light quarks, where spontaneous symmetry breaking by condensates in the vacuum leads to a small mass pion, as well as highly excited states, which are insensitive to this symmetry, yielding parity doublets. Further, measuring the mass splitting between doublets allows determining the quark-mass momentum dependence which connects the asymptotically free current mass to the much larger constituent-quark value. Finally, it has been demonstrated how the Frank-Condon principle can provide information about the quark momentum distribution in heavy quarkonium from decay measurements, some to be performed with the Jefferson Lab 12 GeV upgrade.

Acknowledgements

We thank the organizers for the invitation to discuss these issues at NAPP10 in Dubrovnik. Work supported by grants FPA 2008-00592, FIS2008-01323 plus 227431, Hadron-Physics2 (EU) and PR34-1856-BSCH, UCM-BSCH GR58/08, 910309, PR34/07-15875 and U. S. DOE grant DE-FG02-03ER41260. JMT is a recipient of an FPU scholarship.

References

[1] P. Watson and H. Reinhardt, Phys. Rev. D **77** (2008) 025030.

[2] P. Watson and H. Reinhardt, PoS **Confinement8** (2008) 170.

[3] A. P. Szczepaniak and H. H. Matevosyan, Phys. Rev. D **81** (2010) 094007.

[4] F. J. Llanes-Estrada and S. R. Cotanch, Phys. Rev. Lett. **84** (2000) 1102; see also S. R. Cotanch and F. J. Llanes-Estrada, Fizika B **20** (2011) 1 (this volume).

[5] M. G. Rocha et al., Eur. J. Phys. A **44** (2010) 411.

[6] A. Szczepaniak, C. R. Ji and S. R. Cotanch, Phys. Rev. C **52** (1995) 2738.

[7] G. S. Bali, K. Schilling and A. Wachter, Phys. Rev. D **56** (1997) 2566; in our Coulomb gauge context, see C. Popovici, P. Watson, H. Reinhardt, *Heavy quarks, gluons and the confinement potential in Coulomb gauge,* [arXiv:1011.2151 [hep-ph]].

[8] N. Brambilla et al., Rev. Mod. Phys. **77** (2005) 1423.

[9] T. Van Cauteren, P. Bicudo and M. Cardoso et al., Proc. Bonn 2009 Int. Conf. Few Body Physics [arXiv:0912.3418 [hep-ph]].

[10] W. Lucha and F. F. Schoberl, Mod. Phys. Lett. A **5** (1990) 2473.

[11] F. J. Llanes-Estrada, P. Bicudo and S. R. Cotanch, Phys. Rev. Lett. **96** (2006) 081601.

[12] P. Bicudo et al., Phys. Rev. Lett. **103** (2009) 092003.

[13] S. L. Adler and A. C. Davis, Nucl. Phys. B **244** (1984) 469.

[14] L. Y. Glozman, Phys. Lett. B **475** (2000) 329; E. S. Swanson, Phys. Lett. B **582** (2004) 167; C. E. Detar and T. Kunihiro, Phys. Rev. D **39** (1989) 2805.

[15] C. Amsler et al., Phys. Lett. B **667** (2008) 1.

[16] J. M. Torres-Rincon and F. J. Llanes-Estrada, Phys. Rev. Lett. **105** (2010) 022003.

[17] A. Drutskoy et al. [Belle Collaboration], Phys. Rev. D **81** (2010) 112003.

UZBUDNI HADRONSKI SPEKTAR U QCD COULOMBOVOJ BAŽDARNOSTI

Opisujemo postignuća u razumijevanju uzbudnog hadronskog spektra lakih i teških kvarkova u okviru QCD Coulombove baždarnosti. Za sustave lakih kvarkova ističemo neosjetljivost na spontano lomljenje kiralne simetrije, što predskazuje Wignerovu degeneraciju po parnosti hadronskog spektra visoke uzbude i omogućuje mjerenje impulsne ovisnosti o masi kvarka. Za teško-kvarkovske mezonske raspade, uključujemo Franck-Condonovo načelo radi postizanja približnog, ali neovisnog o modelu, shvaćanja strukture na osnovi impulsnih raspodjela čestica u raspadima.